Structural Mapping of the Catalytic Mechanism for a Mammalian Phosphoinositide-Specific Phospholipase C[†,‡]

Lars-Oliver Essen,[§,||] Olga Perisic,[§] Matilda Katan,[⊥] Yiqin Wu,[▽] Mary F. Roberts,[▽] and Roger L. Williams*[,§]

Centre for Protein Engineering, MRC Centre, Hills Road, Cambridge CB2 2QH, U.K., CRC Centre for Cell and Molecular Biology, Chester Beatty Laboratories, Fulham Road, London SW3 6JB, U.K., and Merkert Chemistry Center, Boston College, Chestnut Hill, Massachusetts 02167

Received October 7, 1996; Revised Manuscript Received December 12, 1996[⊗]

ABSTRACT: The crystal structures of various ternary complexes of phosphoinositide-specific phospholipase C-δ1 from rat with calcium and inositol phosphates have been determined at 2.30−2.95 Å resolution. The inositol phosphates used in this study mimic the binding of substrates and the reaction intermediate and include D-*myo*-inositol-1,4,5-trisphosphate, D-*myo*-inositol-2,4,5-trisphosphate, D-*myo*-inositol-4,5-bisphosphate, and D,L-*myo*-inositol-2-methylene-1,2-cyclicmonophosphonate. The complexes exhibit an almost invariant mode of binding in the active site, each fitting edge-on into the active site and interacting with both the enzyme and the catalytic calcium at the bottom of the active site. Most of the active site residues do not undergo conformational changes upon binding either calcium or inositol phosphates. The structures are consistent with bidentate liganding of the catalytic calcium to the inositol phosphate intermediate and transition state. The complexes suggest explanations for substrate preference, pH optima, and ratio of cyclic to acyclic reaction products. A reaction mechanism is derived that supports general acid/base catalysis in a sequential mechanism involving a cyclic phosphate intermediate and rules out a parallel mechanism where acyclic and cyclic products are simultaneously generated.

Mammalian phosphoinositide-specific phospholipases C (PI-PLC, EC 3.1.4.11)[1] catalyze hydrolysis of phosphatidylinositol-4,5-bisphosphate (PIP_2) to D-*myo*-inositol-1,4,5-trisphosphate (1,4,5-IP_3) and *sn*-1,2-diacylglycerol (DAG) (Rhee & Choi, 1992; Lee & Rhee, 1995). Both products of this reaction function as second messengers in eukaryotic signal transduction cascades. The soluble product 1,4,5-IP_3 triggers inflow of calcium from intracellular stores (Berridge, 1993). The membrane-resident product diacylglycerol controls cellular protein phosphorylation states by activating various protein kinase C isozymes (Dekker et al., 1995).

Three classes of mammalian PI-PLCs with 10 different isozymes have been characterized ($\beta1-\beta4$, $\gamma1-\gamma2$, $\delta1-\delta4$). The activity of β- and γ-isozymes is regulated by G protein-coupled and tyrosine kinase-linked receptors, respectively (Lee & Rhee, 1995). These isozymes (MW 145−150 kDa) are related to the much smaller δ-isozymes (MW 85 kDa), but in addition to a δ-like core they have protein modules that facilitate their specific interaction with G protein subunits or tyrosine kinase domains. Due to their ubiquitous occurrence in eukaryotes, δ-like isozymes are probably the most ancient form of eukaryotic PI-PLCs and may have coevolved with the appearance of phosphoinositides as membrane components. It is currently not known how δ-isozymes are regulated *in vivo*.

Eukaryotic PI-PLCs are strictly dependent on calcium as a cofactor for enzymatic activity. At physiological calcium concentrations (0.01−10 μM) the substrate preference of eukaryotic PI-PLCs for phosphoinositides is $PIP_2 > PIP \gg PI$ (Ryu et al., 1987). In contrast, bacterial PI-PLCs (MW 35−37 kDa) are metal-independent and hydrolyze only PI and PI-analogues (Griffith et al., 1991). Both eukaryotic and prokaryotic PI-PLCs exert high stereospecificity to the D-*myo* configuration of the inositol phospholipid head group (Lewis et al., 1993; Bruzik et al., 1994) but not to the configuration of the C2 position of the diacylglycerol moiety (Bruzik et al., 1992).

An interesting aspect of mammalian PI-PLCs is their ability to form cyclic inositol phosphates as side products of phosphoinositide hydrolysis. The ratio of acyclic to cyclic products depends on the isozyme class ($\gamma > \delta > \beta$), substrate ($PIP_2 > PIP > PI$), pH, and calcium concentration (Kim et

[†] This work was supported by an EU Training and Mobility Fellowship (L.O.E.), the Cancer Research Campaign (M.K.), NIH Grant GM-26762 (M.F.R.), British Heart Foundation (R.L.W.) and the MRC/DTI/ZENECA/LINK Programme (R.L.W.).

[‡] X-ray coordinates and structure factors have been deposited in the Brookhaven Protein Data Bank under the accession numbers 1DJX, 1DJY, 1DJW and 1DJZ for the PLC-δ1 complexes with 1,4,5-IP_3, 2,4,5-IP_3, $cICH_2P$, and 4,5-IP_2.

* Author to whom correspondence should be addressed. FAX: 44-1223-402 140. Tel: 44-1223-402 171. E-mail: rlw@mrc-lmb.cam.ac.uk.

[§] MRC Centre.

[||] Current address: Max Planck Institute for Biochemistry, Department of Membrane Biochemistry, Am Klopferspitz 18a, D-82152 Martinsried bei München, Germany.

[⊥] Chester Beatty Laboratories.

[▽] Boston College.

[⊗] Abstract published in *Advance ACS Abstracts,* February 1, 1997.

[1] Abbreviations: CHAPSO, 3-((3-cholamidopropyl)dimethylammonio)-2-hydroxy-1-propanesulfonate; cIP, D-*myo*-inositol 1,2-cyclic-monophosphate; cIP_3, D-*myo*-inositol 1,2-cyclic 4,5-trisphosphate; $cICH_2P$, *myo*-inositol-2-methylene-1,2-cyclic-monophosphonate; CVFF, consistent valence forcefield; DAG, *sn*-1,2-diacylglycerol; di-C_4-PI, 1,2-dibutyryl-*sn*-glycero-3-phosphoinositol; GST, glutathione-S-transferase; 1,4,5-IP_3, D-*myo*-inositol 1,4,5-trisphosphate; 2,4,5-IP_3, D-*myo*-inositol 2,4,5-trisphosphate; 1,3,4,5-IP_4, D-*myo*-inositol 1,3,4,5-tetraphosphate; IPTG, isopropyl β-D-thiogalactopyranoside; PC, phosphatidylcholine; PH domain, pleckstrin homology domain; PI, phosphatidylinositol; PIP, phosphatidylinositol 4-monophosphate; PIP_2, phosphatidylinositol 4,5-bisphosphate; PIP_3, phosphatidylinositol 3,4,5-trisphosphate; PI-PLC, phosphoinositide-specific phospholipase C; PMSF, phenylmethylensulfonyl fluoride; TIM, triosephosphate isomerase.

S0006-2960(96)02512-3 CCC: $14.00

Scheme 1

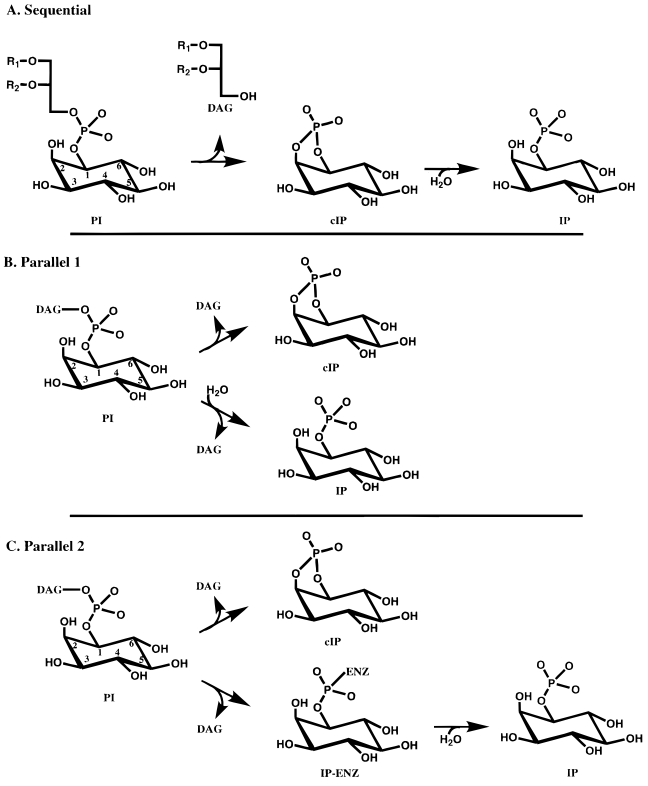

al., 1989). Two major models have been proposed to explain the simultaneous presence of phosphotransferase and phosphohydrolase activity in PI-PLCs (Bruzik & Tsai, 1994): parallel reaction mechanisms in which cyclic and acyclic products are formed simultaneously and a sequential mechanism in which the cyclic inositol represents a reaction intermediate. In one parallel mechanism (Scheme 1), a competitive attack by water and the axial 2-OH group of the D-*myo* inositol group on the phosphodiester group was suggested assuming that the enzyme indiscriminately activates water and the 2-hydroxyl for attack or exists in two conformational states with different activities (Dawson et al., 1971; Lin et al., 1990). However, this mechanism is not consistent with stereochemical data showing retention of the configuration at 1-phosphorus in the acyclic product (Bruzik et al., 1992). An alternative parallel double-displacement mechanism that is consistent with stereochemical data proposed formation of a covalent enzyme−inositol phosphate intermediate as a requirement for acyclic product formation. The sequential mechanism is similarly consistent with these stereochemical data. This mechanism was demonstrated for the bacterial PI-PLC from *Bacillus cereus* (Scheme 1) where the formation of 1,2-cyclic inositol phosphate as a reaction intermediate was experimentally shown (Volwerk et al., 1990; Bruzik et al., 1992). In contrast to eukaryotic PI-PLCs which predominantly generate acyclic products, the bacterial enzyme forms cyclic inositol phosphate (cIP) as the main product under physiological conditions with hydrolysis of cIP proceeding only slowly.

Kinetic studies on mammalian PI-PLCs showed a processive mode of catalysis on the membrane surface (Wahl et al., 1992; Cifuentes et al., 1993; James et al., 1995). Processivity of PLC-δ1 relies on the presence of an N-terminal PH domain that mediates tethering of the enzyme to the lipid membrane (Cifuentes et al., 1993; Paterson et al., 1995). The PH domain (residues 1−132) carries a noncatalytic binding site for the substrate PIP_2, and its structure was recently solved in a complex with 1,4,5-IP_3 (Ferguson et al., 1995a). Structural work on the remaining, catalytically active portion of PLC-δ1 from rat revealed the complete domain organization of PLC-δ1 and gave numerous insights into its mode of action (Essen et al., 1996). The catalytic site is part of a TIM-barrel-like domain (residues 299−606) that is connected at its C-terminus with a putatively membrane-binding C2 domain (residues 626−756) and at its N-terminus with an EF-hand domain (residues 133−289). A catalytic calcium ion was found to be part of the active site, although additional noncatalytic calcium sites were identified in the C2 domain. Most of the residues identified to be relevant for binding of the substrate or catalytic calcium ion reside in the first half of the TIM-barrel-like domain. This region exhibits high structural similarity with the bacterial enzyme, indicating evolutionary relationship between eukaryotic and prokaryotic PI-PLCs.

In this report, we focus on the structural requirements for the chemical steps of PI-PLC catalysis. As a strategy, we soaked PLC-δ1 crystals with compounds which model the reaction course by having different phosphorylation states at the 1- and 2-hydroxyl groups (Figure 2). Crystal structures of PLC-δ1/Ca^{2+} complexes with inositol 2,4,5-trisphosphate, inositol 4,5-bisphosphate, and inositol-2-methylene cyclic-1,2-monophosphonate were solved and refined at maximal resolutions of 2.45−2.95 Å. Together with a further refined 2.3 Å structure of a PLC-δ1/Ca^{2+}/1,4,5-IP_3 complex (Essen et al., 1996) these structures allow us to map most of the reaction pathway, productively bound substrate, transition state, cyclic and acyclic products, and to elucidate the role of the catalytic calcium ion. Finally, this set of structures rules out parallel mechanisms in favor of a sequential mechanism with cyclic inositol phosphate as a reaction intermediate.

EXPERIMENTAL PROCEDURES

Purification, Crystallization, and Crystal Soaking

The expression and purification of Δ(1−132) PLC-δ1, a catalytically active deletion variant that lacks the N-terminal PH domain, were performed using a protocol that is an optimized variant of a previously reported one (Ellis et al., 1993). 12 L of 2× TY/Amp was inoculated 1:100 with an overnight culture of *Escherichia coli* strain HB101 harboring the expression plasmid ME10 for the GST/Δ(1−132) PLC-δ1 fusion. Cells were grown at 34 °C, induced at an OD_{600} $\approx$ 0.5 with 0.1 mM IPTG, and grown for 12 h at 23 °C. Cells were pelleted, sonicated in cold buffer A (PBS, 1 mM EDTA, 1% v/v Triton X-100, 2.5 mM DTT, 0.2 mM PMSF), and centrifuged at 20000*g* for 30 min at 4 °C. The supernatant was incubated for 1 h with 6 mL of glutathione-Sepharose beads at 4 °C. Beads were thoroughly washed with (1) buffer A + 0.3 M NaCl, (2) buffer A without PMSF, (3) PBS, and finally (4) 50 mM Tris·HCl, pH 8.0, 175 mM NaCl. In the last buffer, bound GST fusion protein was cleaved with 0.5 NIH unit of thrombin per mg of fusion protein for 45 min at 23 °C. Beads were separated from the supernatant by centrifugation, and the thrombin reaction was stopped by adding 0.2 mM PMSF to the supernatant. Beads were washed with 25 mL of AQ buffer (20 mM Tris·HCl, pH 8.0, 0.1 mM EGTA, 1 mM DTT). The

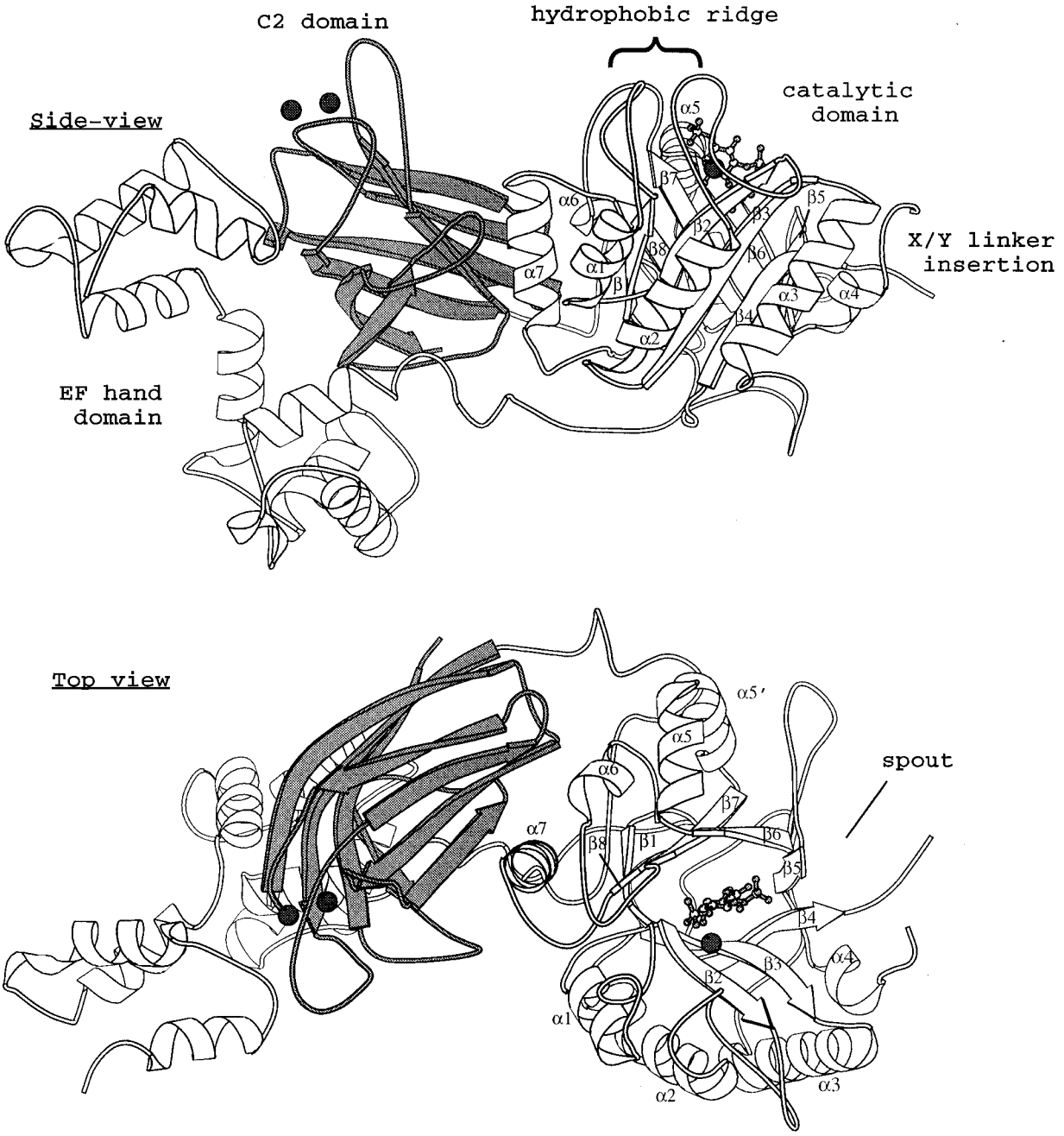

FIGURE 1: Overall structure of the Δ(1−132) deletion variant of phospholipase C-δ1 from rat. The C-terminal C2 domain is shaded to clarify the domain boundaries. The "top" view approximately corresponds to a view from the membrane surface. The bound calcium in the active site is shown as a sphere, and 1,4,5-IP_3 in the active site is represented in ball-and-stick form. The positions of calcium binding sites in the C2 domain are also indicated as spheres. This diagram and Figures 3 and 4A−7A were generated using MOLSCRIPT (Kraulis, 1991).

supernatant was applied onto a MonoQ 10/10 column equilibrated in AQ buffer. Protein was eluted at 0.15 M NaCl. The pooled fractions were concentrated and applied to a Superdex75 16/60 column equilibrated with a buffer containing 10 mM Tris·HCl, pH 8.0, 100 mM NaCl, 0.5 mM EGTA, 1 mM DTT, and 0.01% w/v sodium azide.

Cubic PLC-δ1 crystals were routinely generated by microseeding in hanging drops: 2.5 μL of a 10 mg/mL protein solution in storage buffer with 0.1% w/v CHAPSO was added to 2.5 μL of reservoir buffer and then microseeded with 0.5 μL of a 1:10000−1:20000 diluted suspension of a crushed 0.2 mm PLC-δ1 crystal in 2.0 M ammonium phosphate with 1 mM DTT. Drops were equilibrated against 0.75 mL reservoirs of 1.45 M ammonium phosphate, pH 4.75, 1 mM DTT at 12 °C. Typical crystal dimensions were 0.7 mm × 0.5 mm × 0.4 mm.

Crystals were presoaked for at least 22 h in freezing solution consisting of 34% w/v PEG 400, 0.4 M sodium acetate, pH 5.65, in order to wash out CHAPSO. Crystals were then soaked in 95 mM D,L-*myo*-inositol-2-methylene 1,2-cyclic-monophosphonate (5 h), 20 mM inositol 2,4,5-trisphosphate (9 h), or 20 mM inositol 4,5-bisphosphate (5 h) together with 1 mM calcium chloride at 12 °C (for compounds see Figure 2).

X-ray Data Collection and Processing

X-ray data were collected on a 30 cm MAR detector from single frozen crystals at beamline BL4/ID2 of the European

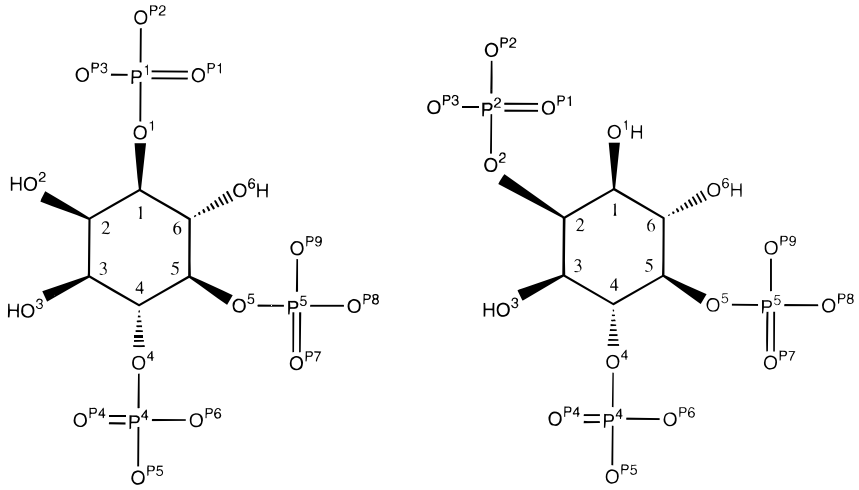

FIGURE 2: Diagram showing the cyclic intermediate cIP and the substrate analogues employed in this study. Soaking experiments with the cIP analogue $cICH_2P$ used a racemic mixture.

Table 1: X-ray Data Collection and Processing

parameter	substrate analogue complexes			
	1,4,5-IP_3	2,4,5-IP_3	$cICH_2P$	4,5-IP_2
space group	$F4_132$	$F4_132$	$F4_132$	$F4_132$
cell dimension (Å)	$a = 397.54$	$a = 397.13$	$a = 397.03$	$a = 396.49$
resolution (Å)	53−2.3	37−2.80	52−2.45	37−2.95
wavelength (Å)	0.890	0.988	0.890	0.988
no. of reflections	755288	396081	495077	326969
no. of unique reflections	113379	59742	95932	55796
R_{merge} (%)[a]	6.2(37.0)	9.4(36.4)	6.7(31.6)	9.1(32.6)
completeness (%)	96.4(94.9)	90.9(91.4)	98.5(97.4)	94.8(92.8)
redundancy	6.7(5.5)	6.6(4.6)	5.2(4.4)	5.9(4.6)
$\langle I/\sigma(I)\rangle$[b]	24.1(5.1)	15.7(4.3)	20.6(4.4)	17.2(4.9)

[a] $R_{merge} = (\sum\sum|I_j(h) - \langle I(h)\rangle|/(\sum\sum I_j(h)) \times 100$; values in parentheses correspond to highest resolution shell. [b] As calculated with the program TRUNCATE (CCP4, 1994).

Synchrotron Radiation Facility (ESRF), Grenoble. A PLC-δ1 crystal in a soaking solution was rapidly frozen in a stream of nitrogen at 100 K. For each data set, a high-resolution and a low-resolution pass were performed due to detector saturation at low resolution. High-resolution passes for PLC-δ1/2,4,5-IP_3 and PLC-δ1/4,5-IP_2 complexes were done with 0.5° oscillations; for PLC-δ1/1,4,5-IP_3 and PLC-δ1/$cICH_2P$ complexes, 0.4° oscillations were used. Low-resolution passes used 1.5° oscillations. The cell dimensions showed a variability of less than 0.5% among different crystals. Raw data were reduced with the MOSFLM (Leslie, 1992) program package. Data scaling and merging were done with the programs SCALA and AGROVATA as implemented in the CCP4 suite (CCP4, 1994). Data statistics are listed in Table 1. Test data for the calculation of free *R* factors of all these data sets were chosen to be consistent with the selection of test data for the native data set (Essen et al., 1996). The test data were selected in thin shells by the program XDLDATAMAN to minimize correlation between the test and working data due to the presence of non-crystallographic symmetry (NCS) in the asymmetric unit (Kleywegt & Jones, 1996).

Table 2: Refinement Statistics

	1,4,5-IP_3[e]	2,4,5-IP_3	$cICH_2P$	4,5-IP_2
resolution	10.0−2.30	10.0−2.80	10.0−2.45	10.0−2.95
R_{factor} (%)[a]	21.7	20.0	21.5	21.2
R_{free} (%)[b]	27.2	25.7	27.0	27.4
no. of reflections	111796	58250	94320	54399
weighted RMSD from ideality[c]				
bond lengths (Å)	0.013	0.016	0.012	0.018
bond angles (deg)	1.378	1.515	1.287	1.640
planarity, trigonal (Å)	0.014	0.015	0.016	0.018
planarity, others (Å)	0.013	0.014	0.013	0.015
torsional angle (deg)	18.706	19.140	18.608	19.440
total no. of atoms	9420	9030	9319	8843
no. of water molecules	840	446	753	269
mean *B* value (Å^2)	42	32	44	31
mean *B* value, protein (Å^2)	41	31	43	31
mean *B* value, solvent (Å^2)	57	38	53	36
mean *B* value, ligands (Å^2)[d]	46	34	48	75

[a] $R = \sum||F_{obs}| - k|F_{calc}||/\sum|F_{obs}|$ with k as scaling factor. [b] Free R factor calculated with 4% of the data not used during refinement. [c] With respect to the Engh and Huber parameters (Engh & Huber, 1991). [d] Including inositol phosphates, calcium ions, and bound acetates. [e] Refinement of the previously described PLC-δ1/1,4,5-IP_3/Ca^{2+} complex (Essen et al., 1996) was extended to 2.3 Å and incorporates an improved solvent model.

Structure Determination and Refinement

Stereochemically restrained least squares refinement was performed with TNT 5E (Tronrud et al., 1987). Stereochemical parameters for the inositol phosphates were derived from CVFF-optimized structures calculated in DISCOVER (Biosym Technologies). The native structure with its two copies of Δ(1−132) PLC-δ1, molecule A and B, served as the starting model (Essen et al., 1996). In the first refinement round, this model was subjected to domain-wise rigid body refinement. A subsequent round of positional and *B* factor refinement was performed without NCS restraints between molecules A and B. Ligands, calcium ions, and a first shell of conserved water molecules were positioned in difference density maps that were calculated with SIGMAA coefficients (Read, 1986) to minimize model bias. The following refinement cycles consisted uniformly of a round of positional and individual *B* factor refinement with NCS restraints, detection of new water molecules in SIGMAA-weighted difference density maps, and manual model adjustment in the graphics program O (Jones et al., 1991). The rebuilding of the solvent sphere was done independently for each of the complex structures. Difference density maps were searched for peaks above 4σ with the programs PEAKMAX and WATPEAKS (CCP4, 1994) and tested if they were found within a distance of 2.2−3.5 Å from a hydrogen bond donor or acceptor. In addition, putative water positions were classified by how close they were to a water molecule in the refined native structure after correcting for differences in domain locations between the native and the complex structures. For this purpose, transformation operators for each domain were derived by superimposing a domain of the complex with the corresponding one of the native structure. Each new water molecule was then mapped onto the native structure by applying the transformation operator of the domain to which it was the closest neighbor. In the first refinement cycles, only conserved water molecules were reintroduced which were closer than 1.4 Å to solvent molecules of the native structure. In subsequent refinement rounds, this criterion was changed to a cutoff radius of 2.1 Å and finally abolished. Water molecules with *B* factors greater than 90 Å^2 after refinement were rejected. Two acetate molecules were located in the interface of the catalytic and the C2 domain around residues Asp 587, Arg 701, and Phe 715 of both molecules. Rebuilding of the solvent sphere was finished after no further drop in the free *R* factor was observed.

The use of a racemic mixture of $cICH_2P$ posed the possibility that actually the L-isomer instead of or in addition to the D-isomer of this analogue for cyclic inositol phosphate is bound in the active site, because the general outlines of both stereoisomers are relatively similar. We modelled both the D- and the L-isomer into the active site and refined both of these models independently. Interpretation of electron density maps with SIGMAA coefficients was consistent with the presence of the D-isomer only, although some negative density in difference density maps around the phosphorus and the exocyclic oxygens of the phosphonate group as well as a high overall *B* factor of 67 Å^2 for $cICH_2P$ suggested partial occupation in the active site. A final optimization of the occupancy for $cICH_2P$ gave an occupancy of 60% in both copies of the PLC-δ1 molecule. The prochiral exocyclic oxygens of its phosphonate group were named O_S and O_R according to the Cahn−Ingold−Prelog nomenclature.

The refinement statistics of all complexes are summarized in Table 2. Due to missing electron density, no structural model was possible for the residues A133−A199, A443−A486, A511−A513, B133−B157, B446−B483, and B511−B513. As in the native model, only EF-hands 3 and 4 (residues 211−281) are completely structurally defined in molecule A. Molecule B shows additionally the C-terminal half of EF-hand 1 (residues 158−175) and the intact EF-hand 2 (residues 176−210). The region 511−513 is part of an extended loop region on the N-terminal side of the catalytic TIM-barrel that connects Tβ5 with Tβ6. The missing residues 446−483 correspond to the XY-linker region, where γ-isozymes have an inserted regulatory multidomain array. Although the stretch of charged residues constituting the XY-linker is located on the C-terminal end of the TIM-barrel and close to the 4,5-phosphoryl binding site of the active site depression, it is dispensable for enzyme activity (Ellis et al., 1993).

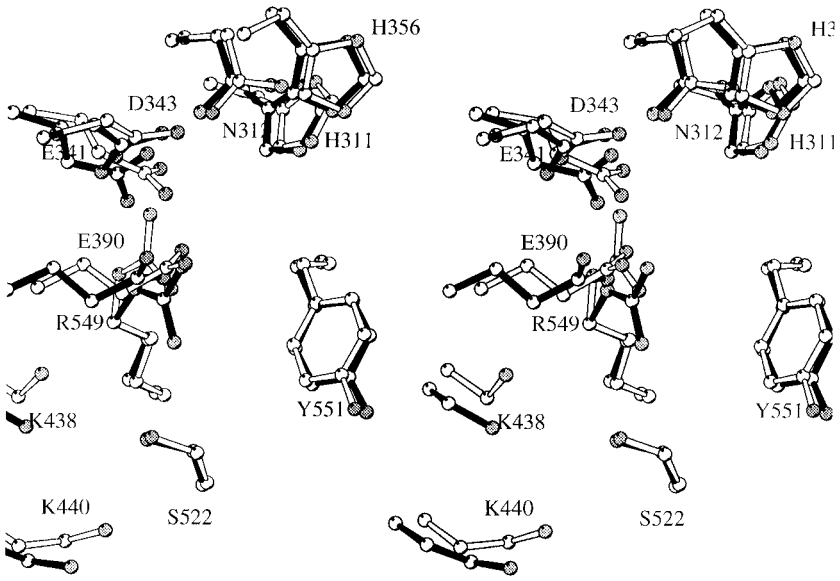

FIGURE 3: Stereorepresentation of the active site residues of the native enzyme (black bonds) superimposed on the active site residues from the 1,4,5-IP_3/Ca^{2+} complex. Carbon atoms are shown as white spheres. Gray-shaded spheres correspond to nitrogen and oxygen atoms.

RESULTS

The crystallization and soaking conditions used in this structural study were close to the pH optimum of 5.5 for PLC-δ1-catalyzed PI hydrolysis. The observed complexes of PLC-δ1 with the various substrate analogues should therefore be relevant for the physiological condition. No significant changes in the orientations of the EF-hand and C2 domains relative to the catalytic domain were observed among the different complexes.

Active Site Geometry

The active site is a broad, solvent-accessible depression on the C-terminal end of the catalytic TIM-barrel (Figure 1). All residues in the active site are strictly conserved among eukaryotic PI-PLCs and, with the exception of the aromatic sidechain of Tyr 551, participate with polar groups in the formation of the active site. A comparison of the active site between the substrate analogue complexes and the native, calcium-free PLC-δ1 structure (Brookhaven Protein Data Bank accession code 1ISD) shows that most of the active site residues do not move upon binding calcium and substrate (Figure 3). Only Glu 341 and Arg 549 exhibit significant structural changes. These residues form a salt bridge with each other at the bottom of the active site. In the native structure, two hydrogen bonds are formed (Glu 341 OE1−Arg 549 NE, 2.7 Å; Glu 341 OE2−Arg 549 NH2, 3.5 Å). Only one of these hydrogen bonds remains in the 1,4,5-IP_3 complex (Glu 341 OE2−Arg 549 NH2, 2.6 Å) after Glu 341 changes from a *gauche*$^-$ conformer for χ_1 ($\chi_1 = -67°$) to a *trans* conformer ($\chi_1 = -169°$). In the 1,4,5-IP_3 complex, the carboxylate oxygen Glu 341 OE1 is a ligand of the catalytic calcium ion and is involved in hydrogen bonds with the 2-OH and 3-OH groups of 1,4,5-IP_3. The guanidinium group of Arg 549 moves about 1.7 Å by an adjustment of the χ_3 torsion angle (166° → −165°). An additional change close to Arg 549 is observed for the conformation of Cys 339 ($\chi_1 = -38° \rightarrow \chi_1 = -174°$), although this highly conserved residue is located under the floor of the active site depression and contacts neither the substrate nor the calcium cofactor. The conformational change enables Cys 339 to interact with Arg 549 by hydrogen-bonding to a bridging water molecule. The only segmental structural move of approximately 0.6 Å is found for the peptide stretch Glu 390−Gln 397 that connects Tβ3 with Tα3. It is probably the result of the carboxyl group of Glu 390 that moves by 0.6 Å closer to the calcium site upon calcium ligation.

The lack of major structural changes upon substrate binding is probably due to "prestabilizing" interactions among active site residues. The conformation of the catalytically important residues His 311 and His 356 is stabilized by an extensive hydrogen-bonding network. The orientation of the side chain of His 311 is fixed by a hydrogen bond between His 311 ND1 and Asn 578 OD1 (2.6 Å). The latter residue is hydrogen-bonded with its ND2 atom to Ser 560 O (2.9 Å) which is located at the outer surface of the TIM-barrel. Similarly, the side chain of His 356 is locked by a hydrogen bond between His 356 ND1 and the backbone oxygen of Gln 319 (2.6 Å). The calcium ligands Asn 312, Asp 343, and Glu 390 are prestabilized by several hydrogen bonds (Asn 312 ND2−Gln 319 OE1, 3.0 Å; Asp 343 OD2−Tyr 314 OH, 2.5 Å; Glu 390 OE2−His 392 NE2, 2.9 Å).

A summary of the interactions between active site residues, the various bound inositol phosphates and calcium can be found in Table 3.

Inositol-1,4,5-trisphosphate Binding

The inositol moiety of the reaction product 1,4,5-IP_3 sits in an edge-on mode in the active site depression (Figures 1 and 4). A network of putative hydrogen bonds and salt bridges between the active site and the bound inositol phosphate ensures that, with the exception of the 6-hydroxyl group, all groups of 1,4,5-IP_3 are stereospecifically recognized. On complexation, half of the 1,4,5-IP_3 surface is buried from solvent access in the active site (119 Å^2 of 253 Å^2). The only major hydrophobic interaction between PLC-δ1 and the 1,4,5-IP_3 molecule is the coplanar stacking of the aromatic ring of Tyr 551 with the inositol ring of 1,4,5-IP_3.

A number of residues conserved within the PI-PLC superfamily have been mutated and several residues, includ-

Table 3: Interatomic Distances in PLC-δ1 Complexes

		distances (Å)[a]							
		1,4,5-IP_3		2,4,5-IP_3		$cICH_2P$		4,5-IP_2	
atom 1	atom 2	A	B	A	B	A	B	A	B
Calcium Coordination									
Asn 312 OD1	Ca^{2+}	2.3	2.5	2.4	2.4	2.5	2.6	2.8	2.7
Glu 341 OE1	Ca^{2+}	2.5	2.6	2.2	2.2	2.6	2.9	2.8	3.1
Asp 343 OD1	Ca^{2+}	2.5	2.4	2.4	2.3	2.4	2.5	2.5	2.7
Asp 343 OD2	Ca^{2+}	2.5	2.3	2.4	2.3	2.5	2.2	2.5	2.3
Glu 390 OE1	Ca^{2+}	2.4	2.3	2.0	1.9	2.9	2.9	2.6	2.8
WAT	Ca^{2+}	3.0	2.7						
Interactions with Substrate Analogue									
Ins O2	Ca^{2+}	2.3	2.2	3.1	2.8			2.2	2.0
Ins O_R	Ca^{2+}					2.8	2.6		
Ins OP2, O_S	Ca^{2+}			2.5	2.3	2.6	2.2		
His 311 NE2	Ins OP1			2.7	2.9				
His 311 NE2	Ins OP2	3.3	2.9						
Asn 312 ND2	Ins O_R					2.7	2.5		
Asn 312 ND2	Ins OP2	2.9	2.6	2.8	2.5				
His 356 NE2	Ins OP3	2.9	2.6						
Glu 390 OE1	Ins O_S					2.3	2.4		
Glu 390 OE2	Ins O_S					2.7	2.9		
Glu 341 OE1	Ins O2	3.0	3.0	3.5	3.1				
Glu 390 OE1	Ins O2	3.0	3.0	3.3	3.1				
Glu 341 OE1	Ins O3	2.7	2.3	3.1	2.5	3.3	3.2	3.4	2.6
Glu 341 OE2	Ins O3	3.1	3.0	2.9	2.8			3.2	3.0
Arg 549 NH1	Ins O3	2.7	2.9	2.6	2.9	2.5	2.7	2.3	2.4
Arg 549 NH1	Ins O4	3.0	3.4	3.0	3.4			3.2	3.0
Lys 438 NZ	Ins OP4	2.6	2.7	2.7	2.9			3.8	2.6
Ser 522 OG	Ins OP4	2.6	2.5	2.3	2.4			2.8	3.3
Arg 549 NH1	Ins OP4	3.0	2.9	3.1	2.8			2.3	2.5
Lys 440 NZ[b]	Ins OP7	4.3	3.9	3.7	3.6				

[a] For each enzyme/ligand distance closer than 3.5 Å, the values are given for PLC-δ1 monomers A and B. [b] Included as putative long-range salt bridge with 5-phosphoryl group.

ing His 311 and His 356, were found to be essential for catalytic activity (Smith et al., 1994; Cheng et al., 1995; Ellis et al., 1995). Although the protonation states of His 311 and His 356 in the crystal are not known it is quite likely that both of them are protonated in the 1,4,5-IP_3 complex, because they form hydrogen bonds with the largely solvent accessible 1-phosphoryl. A distinct feature of IP_3-binding in the active site of PLC-δ1 is the direct coordination of the 2-hydroxyl group to the catalytic calcium ion. In addition, the 2-hydroxyl group is close enough to the calcium ligands Asn 312, Glu 341 and Glu 390 to form hydrogen bonds with their side chains. A similar network of putative hydrogen bonds is found around the 3-hydroxyl group which is in hydrogen-bonding distance to the polar side chains of Glu 341 and Arg 549.

None of the 1-phosphoryl oxygens is engaged in direct liganding to the calcium ion. The closest phosphoryl oxygen, OP2, is 3.8 Å distant from the calcium. An indirect ligation to the calcium is mediated by a bridging water molecule that functions as a calcium ligand (Ca^{2+}−OW, 2.7 Å) and a hydrogen-bonding partner to the phosphoryl atoms OP1 and OP2.

According to the thermal *B* factors the 4-phosphoryl group (34 $Å^2$) shows the lowest degree of structural disorder in the active site followed by the 1-phosphoryl (40 $Å^2$), and the 5-phosphoryl group (49 $Å^2$). The 4- and 5-phosphoryls are located in a pool of water that is contained in this part of the active site depression. The 4-phosphoryl group which is pointing toward the bottom of the active site depression forms *via* its non-bridging oxygen atoms three direct hydrogen bonds with Lys 438, Ser 522, and Arg 549. In addition, several indirect interactions with the enzyme are mediated by intervening water molecules: the 4-phosphoryl group is linked by a water molecule to the side chains of Glu 341 and Ser 388; a water molecule between the 4- and 5-phosphoryls bridges these groups to the hydroxyl group of Ser 501. In contrast to the buried 4-phosphoryl group, the exposed 5-phosphoryl group forms only one salt bridge with Lys 440 and two water-mediated interactions to the hydroxyl groups of Ser 501 and Tyr 551. From the 4- and 5-phosphoryls a continuous water-filled channel projects into the C-terminal widening between β-strands Tβ3 and Tβ4.

Inositol-2,4,5-trisphosphate Binding

In contrast to the 1,4,5-IP_3 complex, the phosphoryl groups in the 2,4,5-IP_3 complex have lower *B* factors. The 2-phosphoryl group shows a highly reduced internal mobility (15 $Å^2$) compared to the 4-phosphoryl (25 $Å^2$) and 5-phosphoryl group (44 $Å^2$). With a torsion angle of 68° for C1−C2−O2−P2 the phosphorus atom of the 2-phosphoryl group is forced to a minimal distance from the 1-hydroxyl group (3.1 Å) by making numerous interactions within the active site (Figure 5). The phosphoryl oxygens OP1 and OP2 are hydrogen-bonded to the side chains of His 311 and Asn 312. The catalytic calcium ion is coordinated in a bidentate manner by the phosphoryl oxygens O2 and OP2. Like in the 1,4,5-IP_3 complex, His 311 is not hydrogen-bonded to the bridging phosphoryl O2 oxygen of this substrate analogue. However, the O2 oxygen is in such a position that it could interact with the calcium ligands Glu 341 and Glu 390. The 4- and 5-phosphoryl groups are bound to the enzyme like in the 1,4,5-IP_3 complex.

$cICH_2P$ Binding

Although being soaked with a racemic D,L-mixture of $cICH_2P$, only the D-isomer was observed in the crystal structure of the PLC-δ1/$cICH_2P$ complex. The partial occupancy of 60% suggests a rather loose mode of binding for this substance. This is probably caused by the lack of 4- and 5-phosphoryl groups in this compound and the subsequent loss of numerous interactions with the active site of the enzyme. The cyclic phosphonate analogue of cIP binds to the catalytic calcium in a bidentate manner with both O_S and O_R exocyclic oxygen atoms of the phosphonate group (Figure 6). The close proximity of the O_S atom to the carboxylate group of Glu 390 indicates the existence of a hydrogen bond and thereby the likely protonation of one of these groups. In addition, the O_R oxygen is forming putative hydrogen bonds to the carboxamide group of Asn 312 and the carboxylate oxygen of Asp 343. The 4- and 5-hydroxyl groups of $cICH_2P$ are not involved in any direct or indirect interactions with the enzyme. The 3-hydroxyl group is hydrogen-bonded to Glu 341 and Arg 549 as in the 1,4,5-IP_3 complex.

4,5-IP_2 Binding

The high average temperature factor for the bound 4,5-IP_2 and especially for its 4- and 5-phosphoryl groups (79 $Å^2$, 100 $Å^2$) suggests a loose binding of this compound to the active site when compared with the 1,4,5-IP_3 and 2,4,5-IP_3 complexes (Figure 7). Like these complexes, 4,5-IP_2 is coordinated with its 2-OH group to the catalytic calcium ion (2.0 Å). The 2-hydroxyl group is within hydrogen-bonding

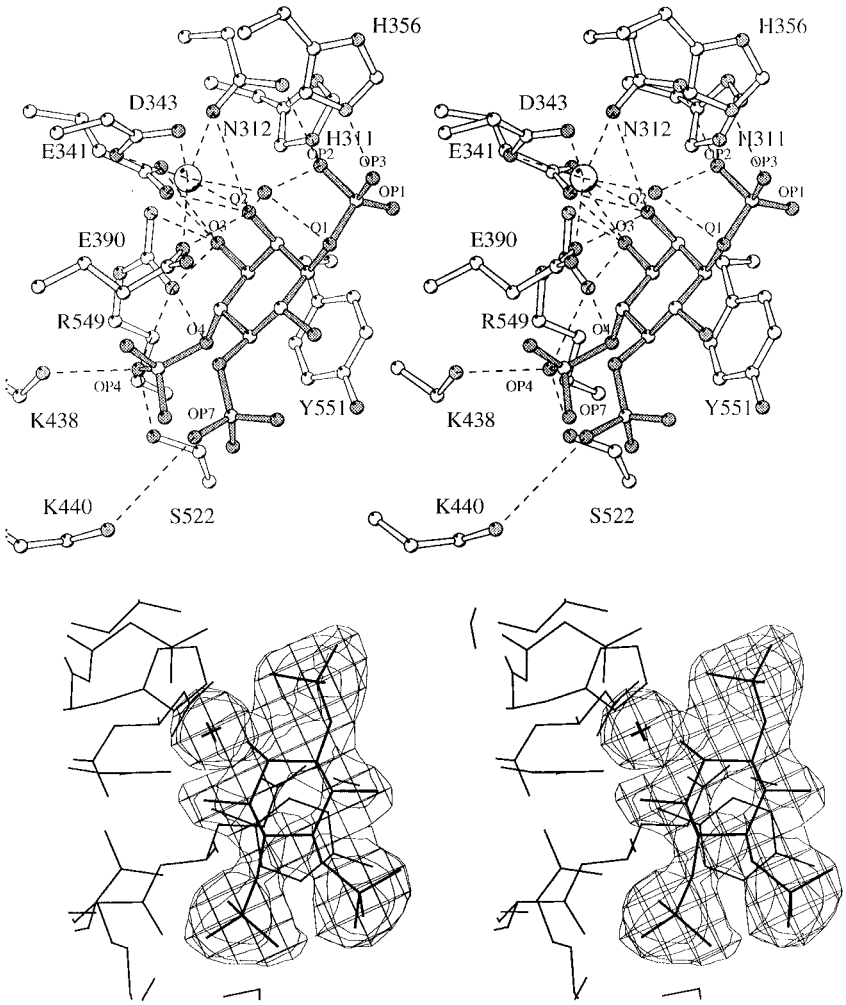

FIGURE 4: Stereoviews of the binding of the reaction product 1,4,5-IP_3 to PLC-δ1. (A) A view of the residues interacting with 1,4,5-IP_3 in the active site. Carbon and phosphorus atoms are depicted as white spheres, oxygens and nitrogens as gray-shaded spheres. All interactions between polar atoms of 1,4,5-IP_3 and the active site (distance < 3.2 Å) are shown as dashed lines. In addition, the putative salt bridge between Lys 440 and the 5-phosphoryl is included. (B) A 2.3 Å resolution $m|F_{obs}| - D|F_{calc}|$ omit map for the 1,4,5-IP_3/Ca^{2+} complex in PLC-δ1 monomer B contoured at 0.2 e/Å^3. Figures 4B−7B were produced with SETOR (Evans, 1993).

distance to Asn 312, Glu 341, and Glu 390. No interaction between the 1-OH group and the enzyme is observed.

Catalytic Calcium Site

The calcium ion sits above β-strand Tβ2 of the catalytic domain complexed to Glu 341 and Asp 343 from this strand and Asn 312 and Glu 390 from the neighboring β-strands Tβ1 and Tβ3. The shorter side chain of Asn 312 is reaching the calcium from the tip of a β-bulge which also accommodates the catalytic residue His 311.

The coordination geometries of the calcium ion vary significantly among the different complexes due to the different participation of substrate atoms in the liganding sphere. In the 1,4,5-IP_3 complex, the geometry can be best described by a regular octahedron where one of the vertices is occupied by the two carboxyl oxygens of Asp 343, three additional vertices by the protein ligands Asn 312 OD1, Glu 341 OE1 and Glu 390 OE1, and the remaining two vertices by a water molecule and the 2-hydroxyl group of 1,4,5-IP_3. In the 2,4,5-IP_3 complex the same ligands are bound to the calcium, but the water molecule is replaced by the OP2 oxygen of the 2-phosphoryl group. The resulting coordination geometry resembles more a square-pyramidal one, where two of the equatorial vertices are occupied by the bidentate ligands Asp 343 and 2,4,5-IP_3, the other two equatorial vertices by Asn 312 and Glu 390, and the apical vertex by Glu 341. A similar, but more distorted geometry is found for the cICH_2P complex. The calcium ion forms with parts of the phosphonate group a four-membered ring by coordinating to the O_S and O_R oxygens. This kind of a bidentate coordination is atypical for the interaction between phosphate groups and Lewis acids, where usually monodentate coordination of the metal ion prevails (Alexander et al., 1990).

The carboxylate groups of Asn 312 and Asp 343 coordinate calcium in a regular geometry typical for small molecule complexes (Einspahr & Bugg, 1981; Carrell et al., 1988). In none of the complexes does the calcium position deviate by more than 1.1 Å from the planes of these carboxyl groups. Regular binding of Glu 341 and Glu 390 to calcium is observed only in the 2,4,5-IP_3 complex. In the 1,4,5-IP_3 and cICH_2P complexes, the calcium coordination by these residues appears to be affected by hydrogen bonds that these residues form with the bound inositol phosphates. The apparent interaction of Glu 390 with the phosphonate oxygen O_S of cICH_2P is probably responsible for the 2.2 Å off-plane deviation of the calcium position from the carboxylate group. Similar off-plane deviations of 1.6 and 2.2 Å are found for

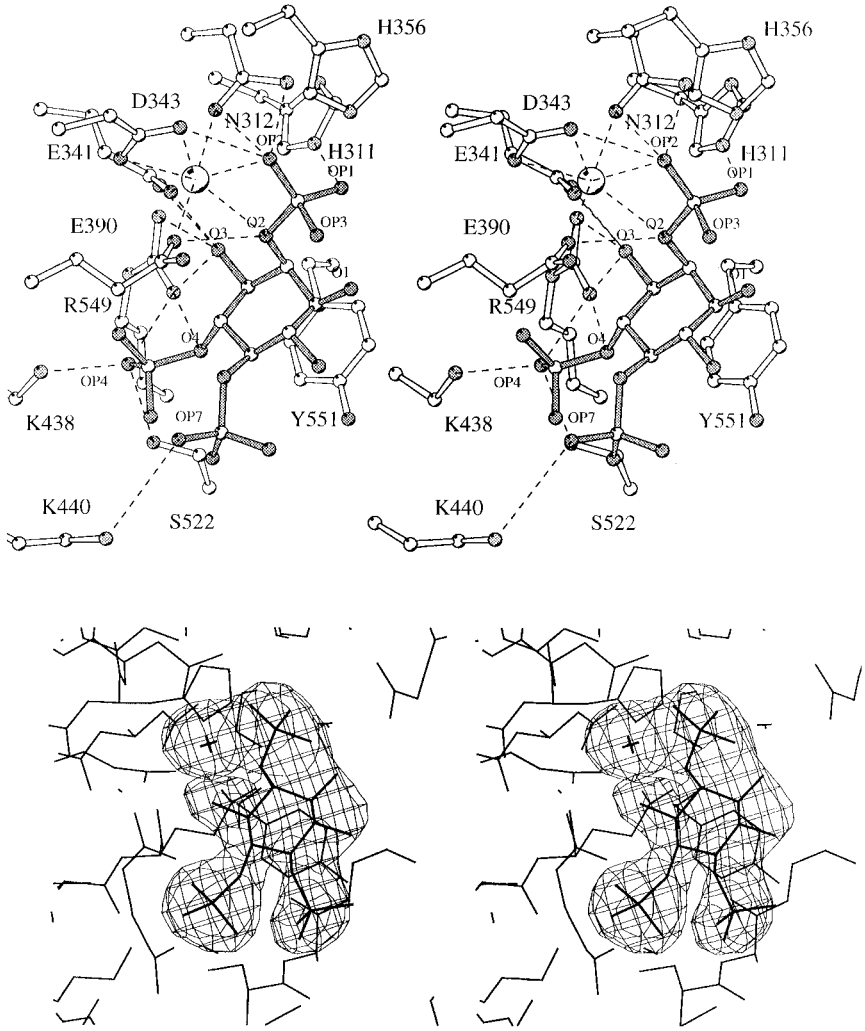

FIGURE 5: Stereoviews of the binding of the substrate analogue 2,4,5-IP_3 to PLC-δ1. (A) A view of active site residues interacting with 2,4,5-IP_3. (B) A $m|F_{obs}| - D|F_{calc}|$ omit map calculated at 2.8 Å resolution for the 2,4,5-IP_3/Ca^{2+} complex in PLC-δ1 monomer B molecule contoured at 0.15 e/Å^3.

Glu 341 and Glu 390 in the 1,4,5-IP_3 complex, where both residues apparently hydrogen-bond to the 2-hydroxyl group. The strong influence of bound substrate analogues on the coordination sphere of the catalytic calcium can also be seen from binary complexes of PLC-δ1 with calcium or calcium analogues (Essen et al., 1997). In these complexes, Glu 341 lacks its hydrogen bonds to the 2- and 3-hydroxyls of bound substrate and is therefore not reoriented toward the calcium, but remains in the conformation of the native enzyme.

DISCUSSION

Binding of Substrates and Substrate Analogues to PLC-δ1

PLC-δ1 has two substrate binding sites: a noncatalytic site in the PH domain and a catalytic site in the TIM-barrel domain. The PH domain tethers the enzyme to PIP_2-containing cellular membranes (Paterson et al., 1995) and is essential for processive catalysis (Cifuentes et al., 1993). The role of the PH domain as a membrane anchor is also reflected by its much higher affinity to PIP_2 ($K_D \approx 1.7$ μM) when compared with the catalytic domain ($K_D > 0.1$ mM). There are two other principal differences between the catalytic and noncatalytic binding site. First, the catalytic domain binds 1,4,5-IP_3 and its analogues with the 2,3,4-edge of the inositol at the bottom of the active site and recognises all chemical groups of IP_3 with the exception of the 6-hydroxyl, whereas the PH domain clamps the 4,5-phosphoryls containing tip of the PIP_2 head group (Ferguson et al., 1995a). These 4- and 5-phosphoryls are probably the most solvent-exposed portion of PIP_2 in lipid membranes due to their highly charged character (Bradshaw et al., 1996) and interaction with them allows the PH domain to skim the surface of the lipid membrane. In contrast, the burial of the lipid head group in the active site positions the scissile phosphodiester bond of the 1-phosphate close to the active site residues and catalytic calcium ion. Second, the PH domain tolerates phosphorylation at the 3-hydroxyl and is consequently capable of binding to PIP_3-containing lipid membranes (Garcia et al., 1995). The catalytic domain cannot accommodate a 3-phosphoryl due to a steric clash with Glu 341 and Arg 549 at the floor of the active site (Williams & Katan, 1996). This is consistent with the inability of PI-PLCs to hydrolyze PIP_3 (Serunian et al., 1989) and represents structurally the focal point for the separation of PIP_2-, PIP_3-, and IP_4-mediated signaling pathways.

Despite these differences, the catalytic and PH domain share some similarities in their interaction with IP_3. Both sites utilize basic and polar residues for interacting either directly or indirectly *via* water bridges with the 4- and 5-phosphoryls. Aromatic side chains of Trp 36 in the PH

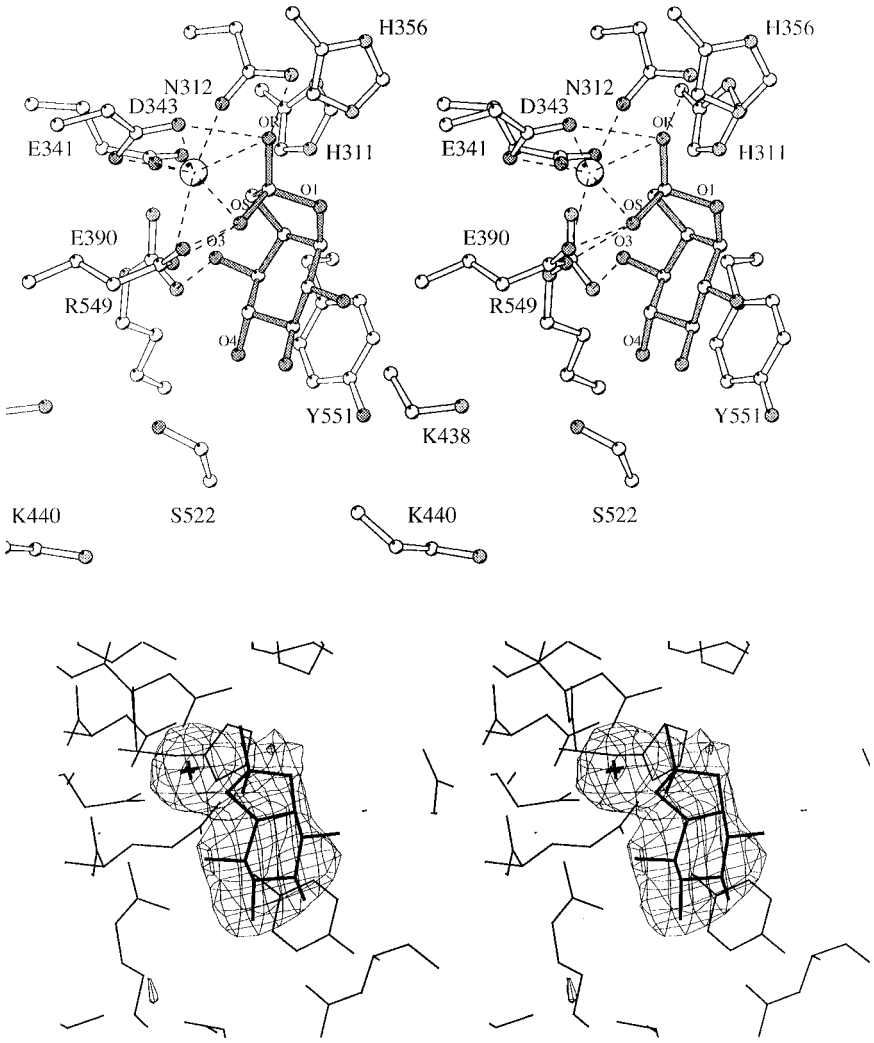

FIGURE 6: Stereoviews of the binding of the cyclic analogue $cICH_2P$ to PLC-δ1. (A) A view of the residues interacting with $cICH_2P$. (B) A $m|F_{obs}| - D|F_{calc}|$ omit map for the $cICH_2P/Ca^{2+}$ complex contoured at 0.15 e/Å^3.

domain and Tyr 551 in the catalytic domain provide numerous van der Waals contacts with the inositol moiety of IP_3. An electrostatic sidedness that was proposed to be responsible for the preferential binding of PH domains to anionic membrane surfaces (Ferguson et al., 1995b) might also be present in the catalytic domain. There is a positively charged surface patch around the binding site of the 4- and 5-phosphoryls (Figure 8) originating from the basic residues Lys 438, Lys 440, and Arg 549 which interact directly with the 4- and 5-phosphoryls and from several other positively charged residues nearby (Lys 441, Lys 485, Lys 487, Lys 500, Arg 530).

The numerous stabilizing interactions between the enzyme and the 4- and 5-phosphoryls of the substrate explain the observed substrate preference of $PIP_2 > PIP \gg PI$ (Ryu et al., 1987). The crucial role of salt bridges between Lys 438, Arg 549 and the 4-phosphoryl group is supported by mutational data (Cheng et al., 1995; Simões et al., 1995). Mutations of Lys 438 or Arg 549 destroyed enzymatic activity toward PIP_2 as substrate. The importance of Arg 549 for substrate specificity was demonstrated by the observation that the mutant enzyme was still active toward PI (Cheng et al., 1995; Wang et al., 1996). The binding of inositol phosphates having phosphoryl groups at the 4- and 5-position is almost invariant. This independence of the binding mode from the phosphorylation status of the 1- and 2-hydroxyl group suggests that there are no reorientations occurring in the active site during the reaction course of PLC-δ1 catalysis.

None of the complexes described here contain the diacylglycerol portion of the native substrates. In contrast to phospholipase A_2 and PC-PLC enzymes, PI-PLCs do not have any preference for the configuration at the C2 atom of the DAG moiety (Bruzik et al., 1992), nor do they have a hydrophobic cleft like that found in phospholipase A_2 (Scott et al., 1990). This suggests that PI-PLCs make only limited interaction with the DAG moiety. However, kinetic studies of lipid substrates with short acyl chains at concentrations below the critical micellar concentration (Rebecchi et al., 1993) indicate that the efficiency with which substrates are hydrolyzed is profoundly increased with increasing acyl chain length. A convex hydrophobic ridge located at one end of the active site opening that consists of three loops connecting Tβ1 with Tα1, Tβ2 with Tα2, and Tβ7 with Tα6 was shown to bind the hydrophobic portion of a detergent (Essen et al., 1996). During catalysis on a membrane surface the ridge could partially penetrate into the aliphatic portion of the membrane. Further structural studies with substrates having an intact diacylglycerol moiety will be necessary to determine what interactions diacylglycerol may form with the enzyme.

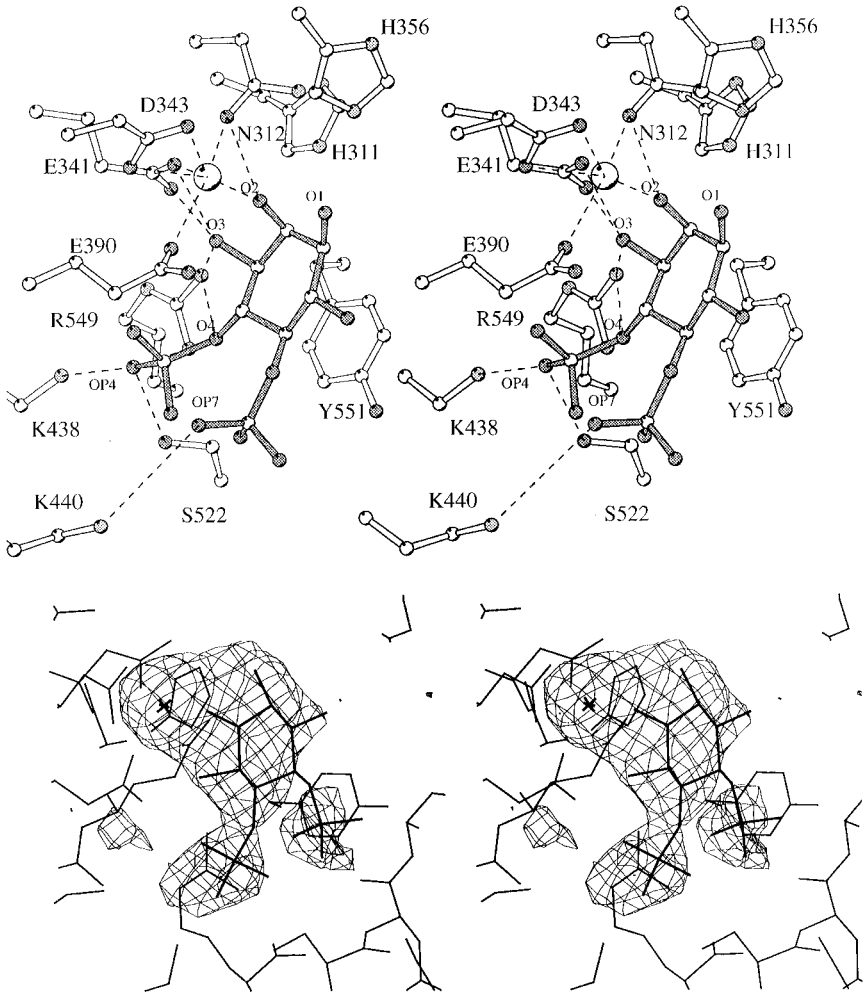

FIGURE 7: Stereoviews of the binding of the substrate analogue 4,5-IP_2 to PLC-δ1. (A) A view of the residues interacting with 4,5-IP_2. (B) A $m|F_{obs}| - D|F_{calc}|$ omit map for the 4,5-IP_2/Ca^{2+} complex contoured at 0.10 e/Å^3.

No measurements of affinities for any of the phospholipid head group or intermediate analogues we have employed are available. However, kinetic measurements with related compounds such as di-C_4-PI (Rebecchi et al., 1993) and glycerophosphoinositides (Y. Wu, O. Perisic, R. Williams, and M. Roberts, unpublished data) suggest affinities in the millimolar range. Because of the rather low affinities, compounds lacking particular interacting groups may result in partial occupancies or higher than average temperature factors, such as seen with the 4,5-IP_2 and $cICH_2P$ in comparison with the inositol trisphosphates.

Structural data of a binary PLC-δ1/Ca^{2+} complex show that the binding of calcium to the catalytic site occurs also in the absence of bound substrate (Essen et al., 1997). The binding of the catalytic calcium might therefore precede and facilitate the binding of substrate. In addition to substrate binding by liganding the 2-hydroxyl group, calcium may also neutralize the acidic cluster Glu 341, Asp 343, and Glu 390 to allow the highly negatively charged PIP_2 head group to bind.

One enzymological feature of mammalian PI-PLCs is the shift of the pH-optimum from pH 7.0−7.5 for PIP_2 or PIP hydrolysis to pH 5.0−5.5 for PI hydrolysis. There are two ways in which the presence of additional phosphoryls in the substrate might affect the pH-profile for catalysis. First, PIP_2 binding is probably sensitive to its protonation state. From ^{31}P-NMR studies on PIP_2 in micelles (without protein), apparent pK_as of 7.0 and 7.7 for the protonation of the 4- and 5-phosphoryls, respectively, were derived (Toner et al., 1988). A fully deprotonated 4-phosphoryl would probably interact more strongly with the basic groups of Lys 438 and Arg 549. Alternatively, the binding of PIP_2 or PIP might change the pK_a of a nearby residue acting as a general acid/general base catalyst during the reaction. In the 1,4,5-IP_3 complex, the carboxyl groups of two such candidates, Glu 341 and Glu 390, are only 4.3 Å distant from the 4-phosphoryl group.

A Sequential Nucleophilic Displacement Mechanism

Our set of structures is highly supportive of the sequential double-displacement mechanism involving a cyclic phosphate intermediate which was originally shown for a bacterial PI-PLC (Volwerk et al., 1990) and later proposed for mammalian PI-PLCs on the basis of stereochemical arguments (Bruzik et al., 1992). According to the sequential mechanism (Scheme 1), a 1,2-cyclic inositol phosphate intermediate is formed by an inline attack of the 2-OH group in a phosphotransferase step. In the subsequent phosphohydrolase step, the enzyme-bound cyclic intermediate is hydrolysed by an activated water molecule. The structures of PLC-δ1 complexes with the methylene analogue of cIP, $cICH_2P$, and with the IP_3 isomer 2,4,5-IP_3 provide us with a view of the hypothetical complex with the cyclic reaction intermediate. The enzyme-bound conformation of 2,4,5-IP_3 resembles the

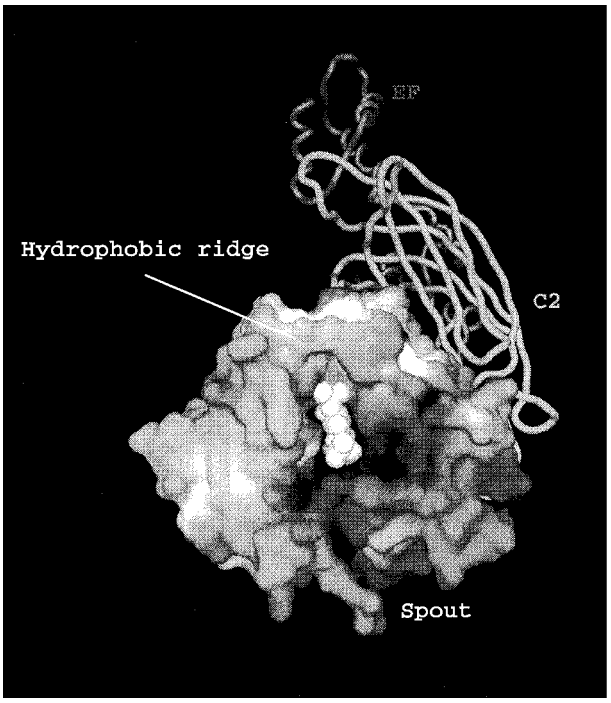

FIGURE 8: "Top" view of the active site. The 1.4 Å probe molecular surface is shaded by electrostatic potential as calculated by GRASP (Nicholls, 1992) assuming charges of +1 for Lys NZ, +0.5 for Arg NH1 and NH2, −0.5 for Asp OD1 and OD2, −0.5 for Glu OE1 and OE2, and +2 for calcium with all other atoms neutral. Black surface shading corresponds to positively charged regions (+14 kT_{298}/e), and white shading to negatively charged ones (−14 kT_{298}/e).

structure of cIP_3, because the 2-phosphorus atom differs in its location by only 0.6 Å from that of an energy-optimized cIP_3 structure, whereas the 1-phosphorus position of the complex with the reaction product 1,4,5-IP_3 deviates by more than 2.0 Å. This new structural information is incorporated into a detailed reaction mechanism for PLC-δ1 as summarized in Figure 9. This mechanism is essentially an extended version of a recently proposed mechanism that relied exclusively on information derived from the 1,4,5-IP_3 complex (Essen et al., 1996).

Early parallel mechanisms supposed a competitive attack of an activated water instead of the inositol 2-hydroxyl group on the phosphodiester (Dawson et al., 1971). Although this mechanism appears to be compatible with the structure of the PLC-δ1/1,4,5-IP_3 complex where a calcium-liganded water molecule is close to the 1-phosphoryl group, it clearly contradicts the observed retention of 1-phosphoryl configuration on formation of acyclic inositol phosphates by PLC-β1 (Bruzik et al., 1992). The alternative parallel mechanism which is consistent with the stereochemical data and involves a covalent histidine−inositol phosphate intermediate can be ruled out on the basis of our complex structures, because neither His 311 nor His 356 could perform an inline attack on the phosphodiester due to their improper orientations relative to the bound substrate.

Phosphotransfer Step

This first step of the enzymatic mechanism involves nucleophilic attack on the phosphodiester and protonation of the DAG leaving group. From its interaction with the 1-phosphate group, His 356 is predicted to act as the general acid to protonate the DAG group. The first prerequisite for a nucleophilic attack of the 2-hydroxyl group on the phosphodiester is its deprotonation by a general base. The catalytic calcium ion to which the 2-hydroxyl is liganded probably assists in this step by lowering the pK_a of the 2-hydroxyl. Due to several potential general bases around the 2-hydroxyl, the assignment of a chemical group as general base catalyst is ambiguous. In the bacterial PI-PLC from *Bacillus cereus*, the role of the general base was attributed to His 32 (Heinz et al., 1995) which is structurally analogous to His 311 in PLC-δ1. The mutation His 311 Ala leads to more than a 1000-fold reduction in PLC-δ1 activity (Ellis et al., 1995). However, in contrast to the bacterial PI-PLC/*myo*-inositol complex, we observe no hydrogen-bonding of His 311 to the 2-hydroxyl group in any of our complexes. The involvement of this residue in hydrogen bonds with the OP2 oxygen of 1,4,5-IP_3 and the OP1 oxygen of 2,4,5-IP_3 is more consistent with the notion that His 311 is essential for the stabilization of the pentavalent transition state. Alternative candidates for the general base are the calcium ligands Glu 341 and Glu 390. These residues have a geometry suitable for hydrogen bonding to the 2-hydroxyl. Furthermore, Glu 390 forms a salt bridge with the highly conserved residue His 392 that might operate as a charge relay. A proton transfer between either of the glutamate residues and the 2-hydroxyl group would be feasible even in the presence of the positively charged calcium, because any change in the partial charge of the carboxyl group would be compensated by an opposing change at the 2-hydroxyl. A protonated state of Glu 390 might be further stabilised by hydrogen-bonding to the exocyclic phosphate oxygen as exemplified in the structure of the $cICH_2P$ complex, where a short hydrogen bond between the phosphate oxygen O_S and Glu 390 is observed (Figure 6, Table 3). A precedent for such a carboxyl group acting as a metal ligand and a general base might be inositol monophosphatase, a magnesium-dependent enzyme important for the recovery of inositol from inositol phosphates, where structural and mutation data suggest that the magnesium ligand Glu 70 acts as a general base (Bone et al., 1994).

A second prerequisite for an inline attack of the 2-hydroxyl is the proper positioning of the phosphodiester group. Due to the rigid arrangement of the 2-hydroxyl and the 1-phosphate groups in the inositol moiety, formation of a pentavalent transition state requires only a change of the C2−C1−O1−P1 torsion angle from −47° (*gauche*$^-$) in the structure of the 1,4,5-IP_3 complex to 18° (periplanar). The resulting O2−P1 distance of less than 2.3 Å is similar to that for the transition state in the phosphotransfer reaction of ribozymes (Taira et al., 1990). In contrast to the 1,4,5-IP_3 binding, the bulky DAG moiety of acylated substrates might strain the C1-O1 torsion angle more toward the periplanar conformation of the transition state.

In our model of the transition state, the attacking 2-OH and the leaving DAG group occupy the apical positions of a trigonal bipyramid (Figure 9). The highly charged pentavalent transition state is stabilized by various interactions within the active site. Besides the previously discussed His 311-O_R and Glu 390-O_S interactions, an additional hydrogen bond might be formed by the exocyclic O_R oxygen with Asn 312. The O_S oxygen is predicted to ligand to the catalytic calcium ion. The strong stereospecific thio effects of PI-PLCs supports the view that calcium is coordinating the O_S but not the O_R oxygen. Only the R_P isomer of a phosphoro-

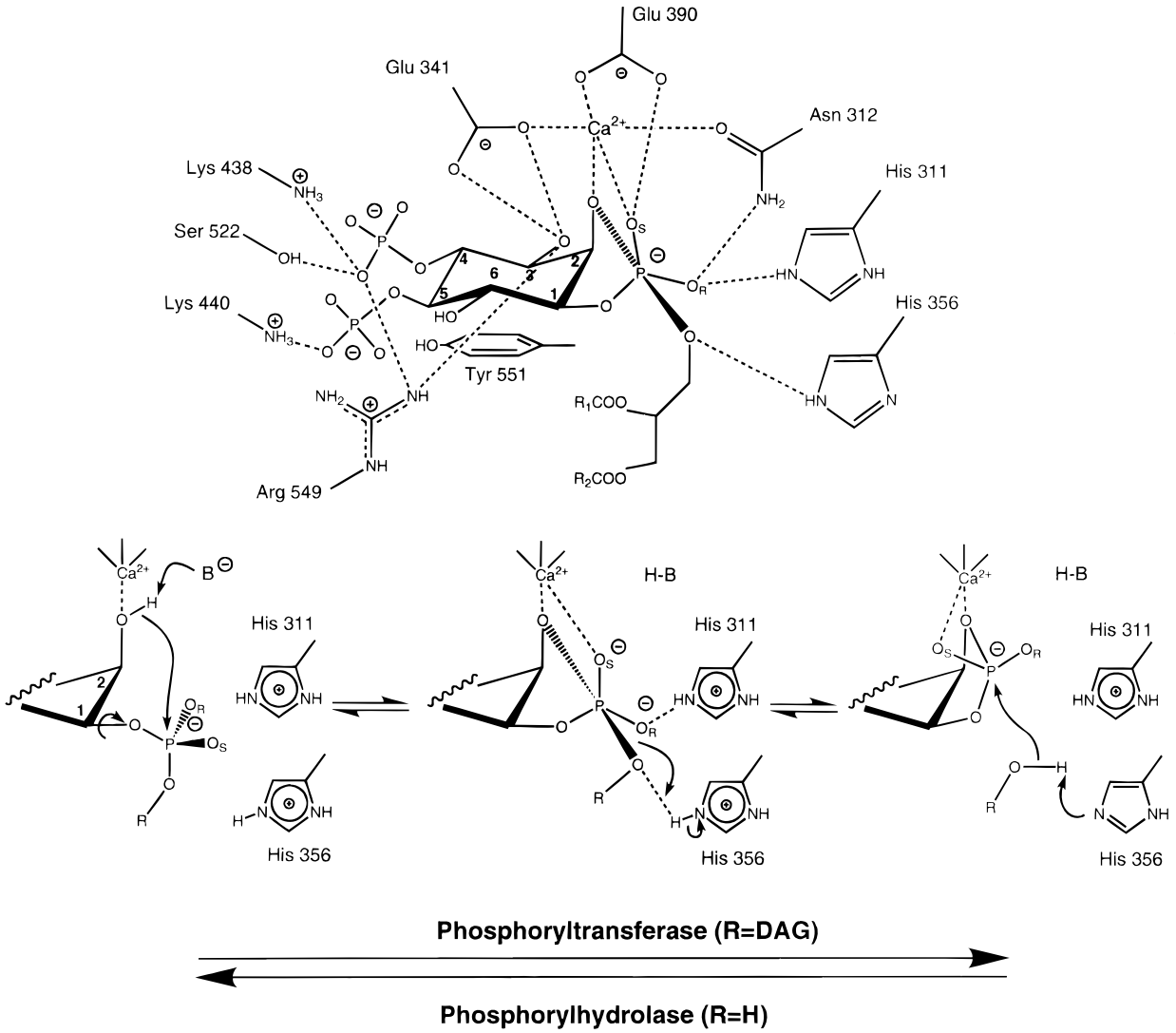

FIGURE 9: Proposed reaction mechanism for PLC-δ1. (A) Schematic representation of the interactions between a hypothetical model of the transition state and the active site of PLC-δ1. Hydrogen-bond formation between Glu 390 and the phosphate oxygen O_S requires protonation of Glu 390. The proton might be derived form the 2-hydroxyl of the substrate (Glu 390 acting as general base) or from another proton donor. (B) Reaction scheme for the general acid/general base catalysis by PLC-δ1. Refer to text for a discussion of the probable identity of the general base (B^-).

thioate analogue of PI is hydrolyzed by mammalian and prokaryotic PI-PLCs (Lin et al., 1990). According to the structural model of the transition state, the thio-substitution of the prochiral O_S oxygen would impair the interaction between the calcium and the phosphate group.

There may be a dual role of the catalytic calcium for accelerating the rate of phosphotransfer in mammalian PI-PLCs. First, calcium should stabilize the negative charge of the deprotonated 2-hydroxyl throughout the reaction course. Second, due to its bidentate mode of liganding the transition state, the calcium might stabilize the transition state relative to the ground state. Both effects, stabilization of the attacking/leaving oxyanion group and preferential binding to the transition state, can have an eminent role for metal-catalyzed phosphotransfer reactions (Herschlag & Jencks, 1987, 1990; Browne & Bruice, 1992).

Phosphohydrolysis Step

The phosphohydrolysis of the enzyme-bound reaction intermediate cyclic IP_3 is proposed to pass through a transition state analogous to the phosphotransfer step. His 356 would thereby generate the attacking hydroxide nucleophile by acting as a general base. Mutation of this residue results in inactivation of the enzyme (Cheng et al., 1995). The role of the catalytic calcium might be slightly different than in the phosphotransfer step. Evidently, it would be capable of stabilizing the leaving 2-hydroxyl in its oxyanionic state, but preferential binding of the transition state might not be expected, because the ground state of this reaction, cIP_3, should already exhibit bidentate or tridentate coordination with its phosphodiester group as seen in the 2,4,5-IP_3 and $cICH_2P$ complexes. However, strain introduced in the cyclic phosphate and cyclohexyl rings would be an additional driving force for ring opening in the phosphohydrolysis step (Bruzik et al., 1996).

Release of Cyclic Inositol Phosphates

One of the most intriguing features of mammalian PI-PLC catalysis is the simultaneous generation of cyclic and acyclic inositol phosphates (Kim et al., 1989). The physiological role of cIP_3 is unclear, although its occurence has been demonstrated in a wide variety of tissues and it apparently can mimic 1,4,5-IP_3 action in various cellular responses (Majerus, 1992). According to the sequential mechanism,

cyclic products are formed by premature release of cyclic inositol phosphate intermediates from the active site. This might be a consequence of the open nature of the active site. In a model of PLC-δ1 docked onto the lipid membrane, the part of the active site which binds the 4- and 5-phosphoryls of the substrate opens like a spout toward the bulk solvent (Figures 1 and 8). This spout would allow diffusion of phospholipid substrates with their head groups into the active site and the release of soluble inositol phosphate products without disturbing the docked enzyme/membrane complex. The efficiency of hydrolysis of cyclic inositol phosphate would therefore be strongly influenced by how well these intermediates are hampered from dilution into the bulk solvent. Accordingly, the higher acyclic to cyclic ratio for PIP_2 or PIP than for PI (Kim et al., 1989) might originate in a slower off-rate of the soluble reaction intermediates from the enzyme due to interactions between the 4- and 5-phosphoryls and the enzyme. The increase of the acyclic/cyclic product ratio at higher pH for PIP and PIP_2 hydrolysis (Kim et al., 1989) might be similarly derived from a stronger binding of higher deprotonated cyclic intermediates or from a higher concentration of the hydroxide nucleophile that would accelerate the phosphohydrolase step.

Calcium As Catalytic Cofactor of PLC-δ1

Although magnesium is a common cofactor for phosphotransfer reactions (Knowles, 1980) and more than 1000-fold abundant in cytosol than calcium, it is not able to replace calcium as catalytic cofactor of mammalian PI-PLC isozymes (Rebecchi & Rosen, 1987). Unlike magnesium, calcium has a high variability for its coordination geometry (McPhalen et al., 1991). The variability is clearly apparent in our complexes where the coordination geometry varies from almost regular octahedral (1,4,5-IP_3 complex) to distorted square-pyramidal (cICH_2P complex). It might be this promiscuity in coordination geometries that is responsible for the essential role of calcium in the PLC-δ1 reaction mechanism, where the substrate/reaction intermediate and the catalytic calcium appear to be rigidly locked in position during the reaction course.

Interestingly, the metal-independent bacterial PI-PLC replaces the catalytic calcium site of the eukaryotic enzyme with basic residues, Arg 69 and Lys 115. The guanidinium group of Arg 69 was proposed to function like calcium in the stabilization of the deprotonated 2-OH nucleophile and/or highly charged pentavalent transition state (Heinz et al., 1995). Further studies will be necessary to clarify whether this difference causes the higher efficiency with which eukaryotic enzymes generate acyclic inositol phosphates as products, i.e., by a slower off-rate of the cyclic intermediate from the active site.

Finally, calcium itself is a major signal of phosphoinositide signalling. The incorporation of calcium not only as a catalytic cofactor of the active site, but also in putative regulatory sites on the C2 and possibly EF-hand domains of PLC-δ1 raises the possibility that calcium exerts feedback regulation on the enzyme activity *in vivo*. It remains for future work to see how the complexity of PI-PLC kinetics, e.g., the exact kinetic role of calcium, is twinned with the complexity of calcium signaling.

ACKNOWLEDGMENT

The authors thank Dr. Robin Irvine for providing a sample of 2,4,5-IP_3, Denise Lynch and Robert Cheng for excellent technical assistance, Dr. Paul Brownlie for help in data collection, Dr. Ian Fearnley for mass spectra of the protein, and the staff of the ESRF synchrotron beamline BL4/ID2 (Grenoble) for their enduring support.

REFERENCES

Alexander, R. S., Kanyo, Z. F., Chirlian, L. E., & Christianson, D. W. (1990) *J. Am. Chem. Soc. 112*, 933−937.
Berridge, M. J. (1993) *Nature 361*, 315−325.
Bone, R., Frank, L., Springer, J. P., Pollack, S. J., Osborne, S. A., Atack, J. R., Knowles, M. R., McAllister, G., Ragan, C. I., Broughton, H. B., Baker, R., & Fletcher, S. R. (1994) *Biochemistry 33*, 9460−9467.
Bradshaw, J. P., Bushby, R. J., Giles, C. C. D., Saunders, M. R., & Reid, D. G. (1996) *Nat. Struct. Biol. 3*, 125−127.
Browne, K. A., & Bruice, T. C. (1992) *J. Am. Chem. Soc. 114*, 4951−4958.
Bruzik, K. S., & Tsai, M.-D. (1994) *Bioorg. Med. Chem. 2*, 49−72.
Bruzik, K. S., Morocho, A. M., Jhon, D. Y., Rhee, S. G., & Tsai, M. D. (1992) *Biochemistry 31*, 5183−5193.
Bruzik, K. S., Hakeem, A. A., & Tsai, M.-D. (1994) *Biochemistry 33*, 8367−8374.
Bruzik, K. S., Guan, Z., Riddle, S., & Tsai, M.-D. (1996) *J. Am. Chem. Soc. 118*, 7679−7688.
Carrell, C. J., Carrell, H. L., Erlebacher, J., & Glusker, J. P. (1988) *J. Am. Chem. Soc. 110*, 8651−8656.
CCP4 (1994) *Acta Crystallogr. D50*, 760−763.
Cheng, H.-F., Jiang, M.-J., Chen, C.-L., Liu, S.-M., Wong, L.-P., Lomasney, J. W., & King, K. (1995) *J. Biol. Chem. 270*, 5495−5505.
Cifuentes, M. E., Honkanen, L., & Rebecchi, M. J. (1993) *J. Biol. Chem. 268*, 11586−11593.
Dawson, R. M., Freinkel, N., Jugalwala, F. B., & Clarke, N. (1971) *Biochem. J. 122*, 605−607.
Dekker, L. V., Palmer, R. H., & Parker, P. J. (1995) *Curr. Opin. Struct. Biol. 5*, 396−402.
Einspahr, H., & Bugg, C. E. (1981) *Acta Crystallogr. B37*, 1044−1052.
Ellis, M. V., U., S., & Katan, M. (1995) *Biochem. J. 307*, 69−75.
Ellis, M. V., Carne, A., & Katan, M. (1993) *Eur. J. Biochem. 213*, 339−347.
Engh, R. A., & Huber, R. (1991) *Acta Crystallogr. 47*, 392−400.
Essen, L.-O., Perisic, O., Cheung, R., Katan, M., & Williams, R. L. (1996) *Nature 380*, 595−602.
Essen, L.-O., Perisic, O., Lynch, D., Katan, M., & Williams, R. L. (1997) *Biochemistry* (in press).
Evans, S. V. (1993) *J. Mol. Graphics 11*, 134−138.
Ferguson, K. M., Lemmon, M. A., Schlessinger, J., & Sigler, P. B. (1995a) *Cell 83*, 1037−1046.
Ferguson, K. M., Lemmon, M. A., Sigler, P. B., & Schlessinger, J. (1995b) *Nat. Struct. Biol. 2*, 715−718.
Garcia, P., Gupta, R., Shah, S., Morris, A. J., Rudge, S. A., Scarlata, S., Petrova, V., McLaughlin, S., & Rebecchi, M. J. (1995) *Biochemistry 34*, 16228−16234.
Griffith, O. H., Volwerk, J. J., & Kuppe, A. (1991) *Methods Enzymol. 197*, 493−502.
Heinz, D. W., Ryan, M., Bullock, T. L., & Griffith, O. H. (1995) *EMBO J. 14*, 3855−3863.
Herschlag, D., & Jencks, W. P. (1987) *J. Am. Chem. Soc. 109*, 4665−4674.
Herschlag, D., & Jencks, W. P. (1990) *J. Am. Chem. Soc. 112*, 1942−1950.
James, S. R., Paterson, A., Harden, T. K., & Downes, C. P. (1995) *J. Biol. Chem. 270*, 11872−11881.
Jones, T. A., Zou, J.-Y., & Cowan, S. W. (1991) *Acta Crystallogr. A47*, 110−119.
Kim, J. W., Ryu, S. H., & Rhee, S. G. (1989) *Biochem. Biophys. Res. Commun. 163*, 177−182.

Kleywegt, G. J., & Jones, T. A. (1996) *Acta Crystallogr. D 52*, 826−828.
Knowles, J. R. (1980) *Annu. Rev. Biochem. 49*, 877−919.
Kraulis, P. J. (1991) *J. Appl. Crystallogr. 24*, 946−950.
Lee, S. B., & Rhee, S. G. (1995) *Curr. Opin. Cell Biol. 7*, 183−189.
Leslie, A. G. W. (1992) *Joint CCP4 and ESF-EACMB Newsletter on Protein Crystallography*, Daresbury Laboratory, Warrington, U.K.
Lewis, K. A., Garigapati, V. R., Zhou, C., & Roberts, M. F. (1993) *Biochemistry 32*, 8836−8841.
Lin, G. L., Bennett, C. F., & Tsai, M. D. (1990) *Biochemistry 29*, 2747−2757.
Majerus, P. W. (1992) *Annu. Rev. Biochem. 61*, 225−250.
McPhalen, C. A., Strynadka, N. C. J., & James, M. N. G. (1991) *Adv. Protein Chem. 42*, 77−143.
Nicholls, A. (1992) *GRASP: Graphical representation and analysis of surface properties*, Columbia University, New York.
Paterson, H. F., Savopoulos, J. W., Perisic, O., Cheung, R., Ellis, M. V., Williams, R. L., & Katan, M. (1995) *Biochem. J. 312*, 661−666.
Read, R. J. (1986) *Acta Crystallogr. A42*, 140−149.
Rebecchi, M. J., & Rosen, O. M. (1987) *J. Biol. Chem. 262*, 12526−12532.
Rebecchi, M. J., Eberhardt, R., Delaney, T., Ali, S., & Bittman, R. (1993) *J. Biol. Chem. 268*, 1735−1741.
Rhee, S. G., & Choi, K. D. (1992) *J. Biol. Chem. 267*, 12393−12396.
Ryu, S. H., Suh, P.-G., Cho, K. S., Lee, K.-Y., & Rhee, S. G. (1987) *Proc. Natl. Acad. Sci. U.S.A. 84*, 6649−6653.
Scott, D. L., White, S. P., Otwinowski, Z., Yuan, W., Gelb, M. H., & Sigler, P. B. (1990) *Science 250*, 1541−1546.
Serunian, L. A., Haber, M. T., Fukui, T., Kim, J. W., Rhee, S. G., Lowenstein, J. M. & Cantley, L. C. (1989) *J. Biol. Chem. 264*, 17809−17815.
Simões, A. P., Camps, M., Schnabel, P., & Gierschik, P. (1995) *FEBS Lett. 365*, 155−158.
Smith, M. R., Liu, Y.-L., Matthews, N. T., Rhee, S. G., Sung, W. K., & Kung, H.-F. (1994) *Proc. Natl. Acad. Sci. U.S.A. 91*, 6554−6558.
Taira, K., Uebayasi, M., Maeda, H., & Furukawa, K. (1990) *Protein Eng. 3*, 691−701.
Toner, M., Vaio, G., McLaughlin, A., & McLaughlin, S. (1988) *Biochemistry 27*, 7435−7443.
Tronrud, D. E., Ten Eyck, L. F., & Matthews, B. W. (1987) *Acta Crystallogr. A43*, 489−501.
Volwerk, J. J., Shashidhar, M. S., Kuppe, A., & Griffith, O. H. (1990) *Biochemistry 29*, 8056−8062.
Wahl, M. I., Jones, G. A., Nishibe, S., Rhee, S. G., & Carpenter, G. (1992) *J. Biol. Chem. 267*, 10447−10456.
Wang, L.-P., Lim, C., Kuan, Y.-S., Chen, C.-L., Chen, H.-F., & King, K. (1996) *J. Biol. Chem. 271*, 24505−24516.
Williams, R. L., & Katan, M. (1996) *Structure 4*, 1387−1394.

BI962512P